

Feasibility of using acoustic scintillation due to underwater turbulence to measure flow speed

Yuen Min Too, Ahmed Mahmood, and Mandar Chitre
Acoustic Research Laboratory, Tropical Marine Science Institute
National University of Singapore, 12A Kent Ridge Road, Singapore 119223
E-mail: {ymtoo, ahmed, mandar}@arl.nus.edu.sg

Abstract—We measure the state of the ocean by exploring the properties of acoustic propagation. One of the approaches, known as acoustic scintillation, exploits the spatiotemporal fluctuation of the propagation to infer information such as turbulent flow within the water. The goal of this study is to investigate the potential of acoustic scintillation by considering only underwater ambient noise. Cross-covariance functions of the received noise amongst the sensors are used to reveal the turbulent flow within the water medium. This in turn describes the environment of our oceans without the need of deploying powerful transmitters that ensonify the underwater medium. Through tank experiments, we demonstrate that acoustic scintillation using random signals can be employed effectively for turbulent flow estimation produced by an air-bubble plume. For comparison, we also employ deterministic narrowband signals and find results in both cases to be supported by video evidence.

I. INTRODUCTION

The idea of estimating the state of the ocean by transmitting a known acoustic signal was first introduced by Munk and Wunsch [1]. The approach, named ocean acoustic tomography (OAT), compares the received signal with that projected by a propagation model. By solving the corresponding inverse problem, information about the intervening ocean such as sound speed profile (SSP), water velocity, etc., can be acquired. Instead of relying on active sound sources, recent studies show that the travel time between two sensors can be extracted solely based on the correlation function of ocean diffuse noise [2], [3]. However, the presence of directional sounds due to shipping and biological activities often results in biased estimates [4]. SSP estimation through matched field processing using unknown acoustic emissions from ships passing within the detection range of the receiver is also shown to be feasible [5]. The aforementioned techniques, passive or otherwise, require an acoustic propagation model well-suited to the measurement area, which may not be known in practice.

In the literature, astrophysicists have constructed atmospheric parameter profiles such as wind motion, turbulent strength, etc., by observing the radiance arriving from the stars [6], [7]. Atmospheric fluctuations essentially cause the stars to twinkle or scintillate. By employing a suitable scattering model, an inverse problem may be solved to determine atmospheric profiles. These concepts have been extended to the underwater domain to measure ocean flow using acoustic waves emitted from known sources [8], [9]. This technique is known as *acoustic scintillation*. Like the OAT, the potential of

acoustic scintillation for long-term ocean monitoring is limited by the high cost of having the signal source. Replacing the active source with ocean ambient sources may be a possible solution.

Ambient noise in the ocean consists of sounds produced by marine organisms (snapping shrimp, marine mammals, etc.), natural physical events (wave, wind, rain, etc.) and human activities (shipping, reclamation, etc). Recent advances in the study of underwater acoustics suggest that the ocean noise can be useful for passive sensing. For example, snapping shrimp noise has been regarded as a consistent and reliable ambient noise source in warm shallow waters for imaging and ecological monitoring [10], [11]. Employing ambient noise as a source of opportunity for acoustic scintillation is still an untapped problem. We perform a preliminary study and investigate the feasibility of underwater flow estimation with various deterministic and random signals over the course of several tank experiments. Our results highlight the practicality of acoustic scintillation in the ocean where ambient noise is always prevalent.

In the rest of this paper, we present a propagation model to describe an acoustic wave propagating through a turbulent flow within the water medium in Section II. By observing the fluctuations of the wave, we show that both the narrowband signal and random signal can be used to estimate the velocity of the turbulence. In Section III, experimental results are shown to verify the findings. Finally, conclusions are drawn in Section IV.

II. PROPAGATION MODEL

An acoustic wave is scattered when it traverses a medium with random inhomogeneities. The scattered waves are superimposed on the primary wave and lead to fluctuations of the primary wave. In the underwater channel, turbulence stirs water properties (such as temperature, salinity, etc.) and/or mixes its contents (such as bubbles, marine biomass, etc.), thus producing random inhomogeneities within. We assume that the turbulence adheres to Taylor's hypothesis, i.e., the rate of change of an eddy is small compared to the velocity of the mean flow. Consequently, the random inhomogeneities move collectively and their relative spatial positions remain constant in time. Theoretical models that explain this phenomena for narrowband signals have been presented in [12], [7], [13]. In this study, through modeling and experimentation, we

$$p(y, z, t) \approx \underbrace{\int_{-\infty}^{\infty} S(\omega) \exp\left(-j\frac{\omega}{c}\sqrt{L^2 + y^2 + z^2}\right) \exp(-j\omega t) d\omega}_{p_0(y, z, t)} - j \underbrace{\int_{-\infty}^{\infty} \phi_{x_l}(\omega, y, z, t) S(\omega) \exp\left(-j\frac{\omega}{c}\sqrt{L^2 + y^2 + z^2}\right) \exp(-j\omega t) d\omega}_{p_1(y, z, t)} \quad (3)$$

investigate the possibility of observing the same phenomena for random signals.

To achieve this end, we now mathematically define our problem. We set up a three-dimensional right-handed Cartesian coordinate system with coordinate point denoted by (x, y, z) . Let an ambient noise source be present at the origin of the coordinate system. The source emits an acoustic wave which propagates through an infinite turbulent layer bounded by the planes $x = x_l$ and $x = x_l + dx$. The acoustic wave is subsequently observed by a receiver on the plane $x = L$ near the x -axis. We assume an iso-velocity channel and a geometric ray model. Fig. 1 illustrates the propagation of the acoustic wave. The acoustic pressure due to the sound source recorded at location $(x = L, y, z)$ and time t can be modeled by [7]

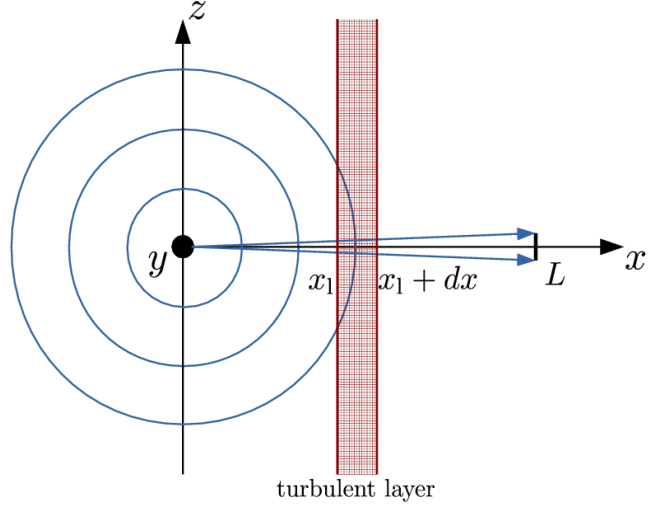


Fig. 1. Acoustic wave propagating through a turbulent layer.

$$p(y, z, t) = \int_{-\infty}^{\infty} S(\omega) \exp\left(-j\left(\frac{\omega}{c}\sqrt{L^2 + y^2 + z^2} + \phi_{x_l}(\omega, y, z, t)\right)\right) \times \exp(-j\omega t) d\omega \quad (1)$$

where $S(\omega)$ is the Fourier coefficient of the emitted acoustic signal samples, $j = \sqrt{-1}$, and c is speed of sound underwater. $\phi_{x_l}(\omega, y, z, t)$ is a complex-valued function of refractive index perturbation $\mu_{x_l}(\omega, y, z, t)$. In the case of weak inhomogeneities, $\mu_{x_l}(\omega, y, z, t)$ is a small value random process which expresses the fluctuations from the mean value such that $\mathbb{E}[\mu_{x_l}(\omega, y, z, t)] = 0$ where $\mathbb{E}[X]$ is the expected value of X . Using Taylor's hypothesis, this function can be written as [7]

$$\phi_{x_l}(\omega, y, z, t) = \frac{\omega}{c} dx \mu_{x_l}\left(\omega, \frac{yx_l}{L} - v_y t, \frac{zx_l}{L} - v_z t\right). \quad (2)$$

v_y and v_z are the mean flow velocities of the turbulence in the y and z axes, respectively.

Since $\phi_{x_l}(\omega, y, z, t)$ is small, (1) can be approximated by (3) at the top of the page. The first term represents the primary wave while the second term is the wave resulting from the scattering of the primary wave due to the turbulence. Since second-order statistics do not converge in several impulsive noise scenarios such as snapping shrimp noise, we use log-square function $\log(a(t)a^*(t))$ to quantify the instantaneous power of $a(t)$ where $*$ is the complex conjugate and $\log(X)$ is natural logarithm of X [14]. We represent the log-square of

the received signal as

$$\begin{aligned} p'(y, z, t) &= \log(p(y, z, t)p^*(y, z, t)) \\ &= \log(p_0(y, z, t)p_0^*(y, z, t)) \\ &\quad + \log\left(1 + \frac{p_0(y, z, t)p_1^*(y, z, t)}{p_0(y, z, t)p_0^*(y, z, t)} + \frac{p_0^*(y, z, t)p_1(y, z, t)}{p_0(y, z, t)p_0^*(y, z, t)}\right. \\ &\quad \left. + \frac{p_1(y, z, t)p_1^*(y, z, t)}{p_0(y, z, t)p_0^*(y, z, t)}\right). \end{aligned} \quad (4)$$

Neglecting the second and higher order smallness of $p_1(y, z, t)$, we have

$$\begin{aligned} p'(y, z, t) &\approx \log(p_0(y, z, t)p_0^*(y, z, t)) \\ &\quad + \frac{p_0(y, z, t)p_1^*(y, z, t)}{p_0(y, z, t)p_0^*(y, z, t)} \\ &\quad + \frac{p_0^*(y, z, t)p_1(y, z, t)}{p_0(y, z, t)p_0^*(y, z, t)}. \end{aligned} \quad (5)$$

Let l be a short time length such that the turbulence is static within l or by definition $\mu(\omega, y, z, t) = \mu(\omega, y, z, t + \delta t)$ for $0 \leq \delta t \leq l$. We divide the signal into multiple fixed-length segments with time length of l . Each segment is indicated by a time index $t_n = nl$ for $n \in \{0, 1, 2, \dots\}$. The intensity of

the signal is given by

$$\begin{aligned} I(y, z, t_n) &= \frac{1}{l} \int_{t_n}^{t_n+l} p'(y, z, t) dt \\ &= I_0(y, z, t_n) + I_1(y, z, t_n) \end{aligned} \quad (6)$$

with

$$I_0(y, z, t_n) = \frac{1}{l} \int_{t_n}^{t_n+l} \log(p_0(y, z, t) p_0^*(y, z, t)) dt \quad (7)$$

as the intensity of the primary wave without random inhomogeneities and

$$\begin{aligned} I_1(y, z, t_n) &= \frac{1}{l} \int_{t_n}^{t_n+l} \frac{p_0(y, z, t) p_1^*(y, z, t)}{p_0(y, z, t) p_0^*(y, z, t)} + \frac{p_0^*(y, z, t) p_1(y, z, t)}{p_0(y, z, t) p_0^*(y, z, t)} dt \end{aligned} \quad (8)$$

as the intensity of the scattered wave due to random inhomogeneities.

Let (L, y, z) and $(L, y + \delta y, z + \delta z)$ be the 3-tuple location coordinates of any two sensors. The temporal cross-covariance function between the signal intensity recorded at the sensors can be expressed as

$$C(\tau) = \mathbb{E}[\tilde{I}(y, z, t_n) \tilde{I}(y + \delta y, z + \delta z, t_n + \tau)] \quad (9)$$

where tilde denotes zero mean, i.e., $\tilde{I} = I - \mathbb{E}[I]$. We expand (9) to become

$$\begin{aligned} C(\tau) &= \mathbb{E}[\tilde{I}_0(y, z, t_n) \tilde{I}_0(y + \delta y, z + \delta z, t_n + \tau)] \\ &\quad + \mathbb{E}[\tilde{I}_0(y, z, t_n) \tilde{I}_1(y + \delta y, z + \delta z, t_n + \tau)] \\ &\quad + \mathbb{E}[\tilde{I}_1(y, z, t_n) \tilde{I}_0(y + \delta y, z + \delta z, t_n + \tau)] \\ &\quad + \mathbb{E}[\tilde{I}_1(y, z, t_n) \tilde{I}_1(y + \delta y, z + \delta z, t_n + \tau)]. \end{aligned} \quad (10)$$

By neglecting the cross terms due to the insignificant values compared to their counterparts, (10) can be approximated by

$$\begin{aligned} C(\tau) &\approx \underbrace{\mathbb{E}[\tilde{I}_0(y, z, t_n) \tilde{I}_0(y + \delta y, z + \delta z, t_n + \tau)]}_{C_0(\tau)} \\ &\quad + \underbrace{\mathbb{E}[\tilde{I}_1(y, z, t_n) \tilde{I}_1(y + \delta y, z + \delta z, t_n + \tau)]}_{C_1(\tau)}. \end{aligned} \quad (11)$$

Note that the cross-covariance function of the received signal intensity is the summation of the cross-covariance functions of the signal intensity without propagation through the turbulence and the scattered signal intensity due to the turbulence. We denote the two cross-covariance functions as $C_0(\tau)$ and $C_1(\tau)$ respectively. For tonals with amplitude A_0 ,

$$\begin{aligned} C^{\text{tonals}}(\tau) &= C_1^{\text{tonals}}(\tau) \\ &= \left(\frac{2\omega dx}{c} \right)^2 \mathbb{E} \left[\text{Im} \left(\mu_{x_l} \left(\omega, \frac{yx_l}{L} - v_y t_n, \frac{zx_l}{L} - v_z t_n \right) \right) \right. \\ &\quad \left. \text{Im} \left(\mu_{x_l} \left(\omega, \frac{(y + \delta y)x_l}{L} - v_y(t_n + \tau), \right. \right. \right. \\ &\quad \quad \left. \left. \left. \frac{(z + \delta z)x_l}{L} - v_z(t_n + \tau) \right) \right) \right] \end{aligned} \quad (12)$$

where $C_0^{\text{tonals}}(\tau) = 0$ and $\text{Im}(X)$ is the imaginary part of X . Note that maximum cross-covariance can be achieved if the time lag τ satisfies $\frac{\delta y x_l}{L} - v_y \tau = 0$ and $\frac{\delta z x_l}{L} - v_z \tau = 0$. Conversely, we are able to estimate the velocities of the turbulence (denoted by (v_y, v_z)) based on the time lag of the main peak of the cross-covariance function. However, having only two sensors does not allow us to satisfy both criteria. Instead of revealing the 2-D mean flow of the turbulence, we can reduce the (y, z) dimensions to $r = \sqrt{y^2 + z^2}$ dimension, and hence we can write $d_r = \sqrt{\delta y^2 + \delta z^2}$, and $v_r = \sqrt{v_y^2 + v_z^2}$. The time lag of the maximum cross-covariance function indicates the 1-D mean flow of the turbulence at the r dimension. The 2-D mean flow of the turbulence can be estimated if there are more than two sensors. For random signals, $C^{\text{random}}(\tau)$ consists of two main peaks. The first peak, which has supports near $\tau = 0$, is caused by $C_0^{\text{random}}(\tau) \neq 0$, an auto-covariance function of $I_0(y, z, t_n)$ as $L \gg \delta y$ and $L \gg \delta z$. Like the tonals, the second peak is due to the fact that same patterns of signal fluctuations have been observed by the two sensors. We construct an experiment to verify the findings.

III. EXPERIMENT

An experiment was conducted in a water tank to investigate the idea of turbulent flow estimation using ambient noise. A transmitter was deployed to mimic the ambient noise source. We considered the following source waveforms:

- 1) 30 kHz, 60 kHz, and 90 kHz tonals to emulate narrow-band noise.
- 2) bandlimited white Gaussian noise (WGN).
- 3) bandlimited α -sub-Gaussian noise (α SGN).

Note that α SGN is an efficient model for snapping shrimp noise. Therefore, the corresponding results for this scenario highlight potential results in warm shallow waters. Due to the hardware limitation of the acoustic sensor, both WGN and α SGN were bandlimited to 10–100 kHz before transmission. All signals were transmitted through an upward rising air-bubble plume acting as a turbulent layer. The propagating signals were received by a two-element vertical linear array. Fig. 2 and 3 show a sketch and a photograph illustrating the layout of the experiment, respectively. The values of the parameters highlighted in Fig. 2, which describe the details of the experimental layout, are stated in Table I. The acoustic pressure recordings of the signals with and without the air-bubble plume are plotted in Fig. 4. Since the characteristics of the acoustic pressure recording of the tonals are similar, we only present the recording of 30 kHz signal. On comparing Fig.4a and 4b, the signal fluctuation due to the propagation through the air-bubble plume is clearly visible. However, the effect of the propagation through air-bubble plume is not obvious for random signals such as WGN and α SGN. From the acoustic pressure recordings, we can easily trace out the intensity frame of the recordings.

The acoustic pressure recordings were preprocessed to signal intensity with the intention to extract the log-square amplitude fluctuations of the received signals. For all transmitted

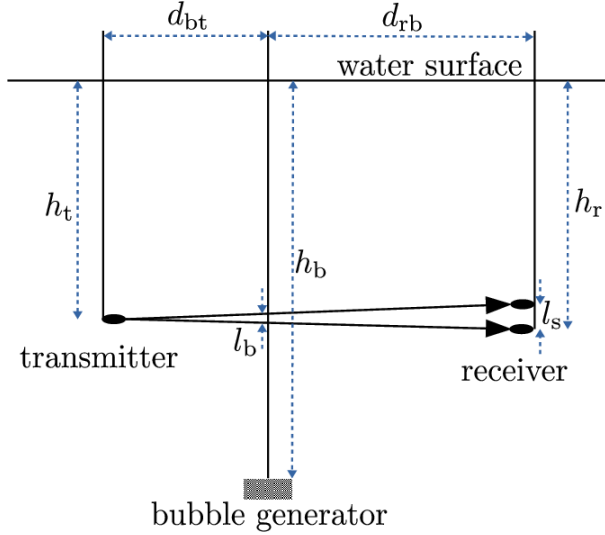


Fig. 2. Schematic of the experimental setup.

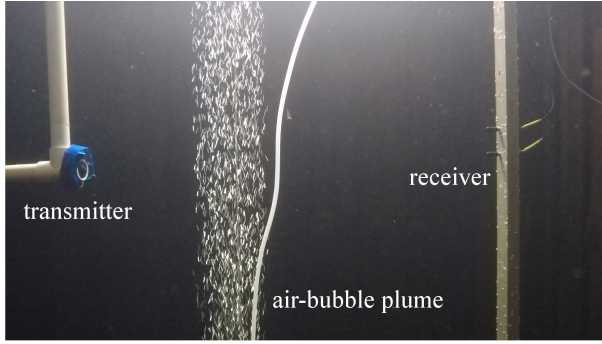


Fig. 3. Photo illustrating the layout of the experiment.

TABLE I
PARAMETERS OF THE EXPERIMENTAL LAYOUT IN MILLIMETERS.

h_r	h_b	h_t	d_{rb}	d_{bt}	l_s	l_b
480.00	1430.00	470.00	500.00	300.00	50.00	18.75

signals, we consider a received sequence of 40 s. The resulting cross-covariance functions are presented in Fig. 5. The cross-covariance curves of each transmitted signal is plotted on the same figure for both cases, with bubbles and without bubbles. The rising speed of the air-bubble plume can be calculated as

$$v_z = \frac{l_s d_{bt}}{(d_{rb} + d_{bt})\tau} = \frac{l_b}{\tau} = \frac{18.75}{\tau} \quad (13)$$

in mm/s where τ (measured in seconds) is the time lag of the main peak of the cross-covariance function. The τ of the correlation functions corresponding to 30 kHz, 60 kHz and 90 kHz signals are 42×10^{-3} s, 48×10^{-3} s and 54×10^{-3} s respectively. According to (13), the estimates of bubble rising speed based on 30 kHz, 60 kHz and 90 kHz signals are approximately 446 mm/s, 391 mm/s and 347 mm/s. For the sake of our study, we consider the average rising speed of

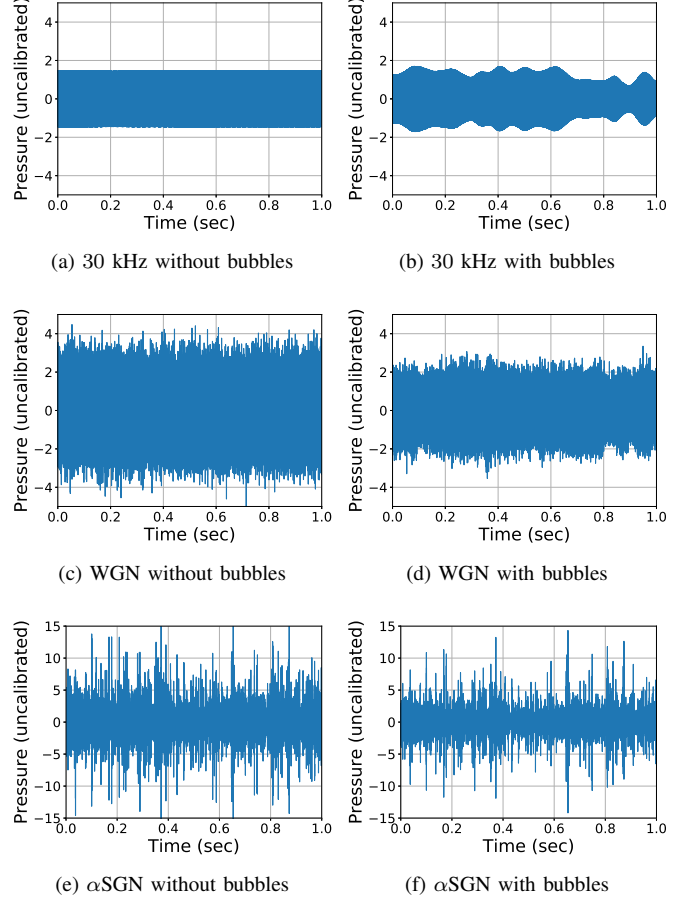


Fig. 4. Acoustic pressure recordings.

the air-bubble plume. This can be interpreted as the average over rise speeds of single bubbles with different sizes. Note that the rise speeds of bubbles depend on their respective sizes. Larger bubbles typically have faster rising speeds [15]. The set of bubbles that weakly scatter the 90 kHz tonal also scatter the 60 kHz and 30 kHz tonals. However, the latter two are also scattered by an increasingly larger set of bubbles of larger size. The estimate of rising speed of the air-bubble plume with respect to the 90 kHz signal is slower because the scattering is dominated by the smaller bubbles with slower rising speed.

For WGN and α SGN, the main peak of the cross-covariance function appears at the zero time lag. This is probably due to the fact that the processing operations are not able to remove the effect from the cross-covariance function of the signal intensity without propagating through the turbulence as discussed in the previous section. By ignoring the nuisance main peak at zero time lag, we notice that there exists a second peak at $30 \times 10^{-3} - 70 \times 10^{-3}$ s time lag as shown in Fig. 5d and Fig. 5e, respectively. This range corresponds to the estimate of the average rising speed of the air-bubble plume in the range of 268 – 625 mm/s. This range tends to agree with the rising speed estimates based on the tonals.

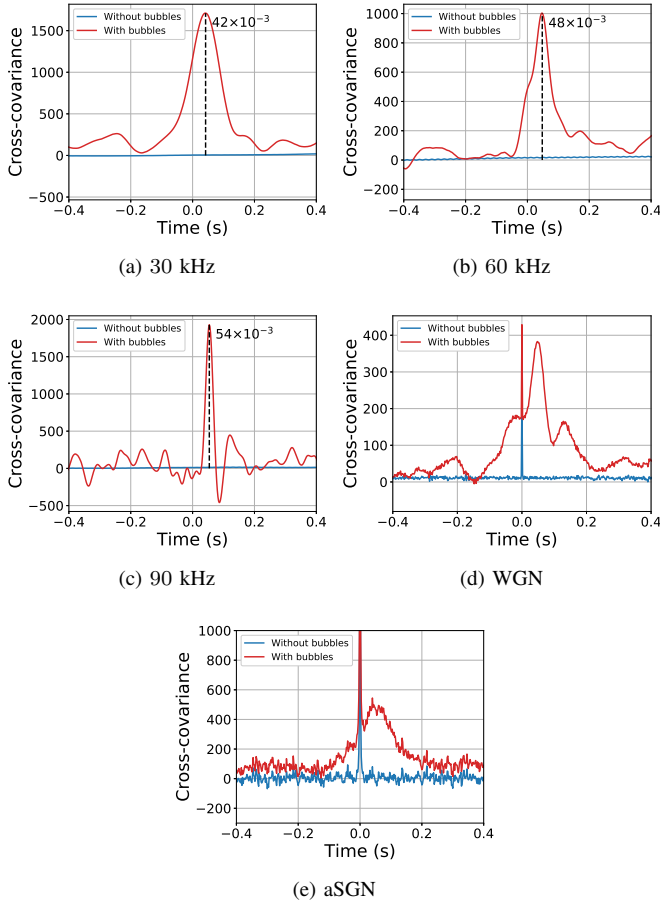


Fig. 5. Cross-covariance functions of the signal intensity without (blue lines) and with (red lines) propagation through the air-bubble plume respectively.

For further verification, we deployed a camera to collect a video of the flow of the air-bubble plume, recorded at 60 frames per second. A frame is shown in Fig. 6. Even though a video frame provides a rough measurement on the vertical displacement of the bubbles, calculating the rising speed of the air-bubble plume based on a large number of video frames is not easy without automated image processing methods for bubble detection and segmentation in each video frame. We computed an average 2-D cross-correlation function of 1200 consecutive video frames as depicted in Fig. 7a. From the 2-D correlation function, we extracted a 1-D cross-correlation function with zero delay at the y-axis denoting the vertical displacement of the air-bubble plume as illustrated in Fig. 7b. The main peak of the 1-D correlation function is positioned at 5.25 mm vertical space lag which is roughly equivalent to the estimate of 315 mm/s the air-bubble plume rising speed. This is consistent with the estimates based on acoustic measurements using narrowband and random signals. All the time lag measurements and the average rising speed are summarized in Table II. The time lag for visual is calculated based on the estimated flow speed of 315 mm/s and the distance of 18.75 mm.

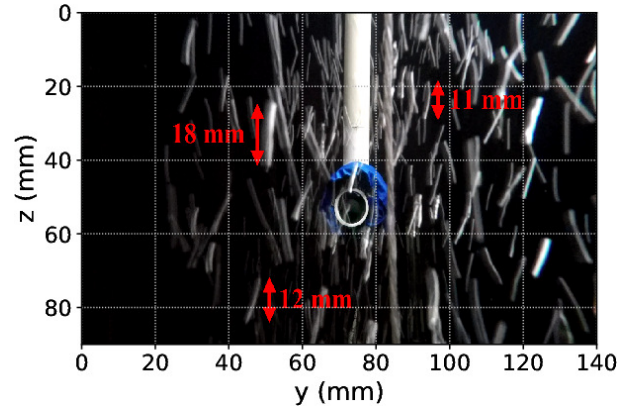
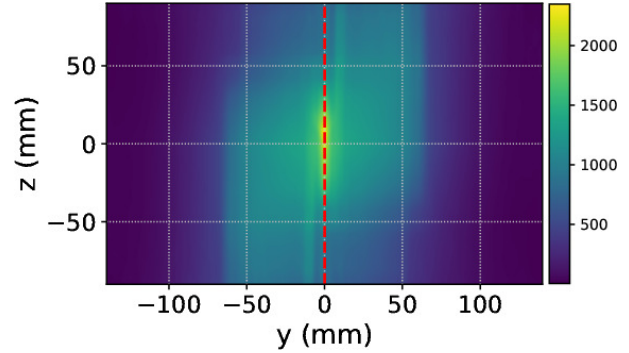
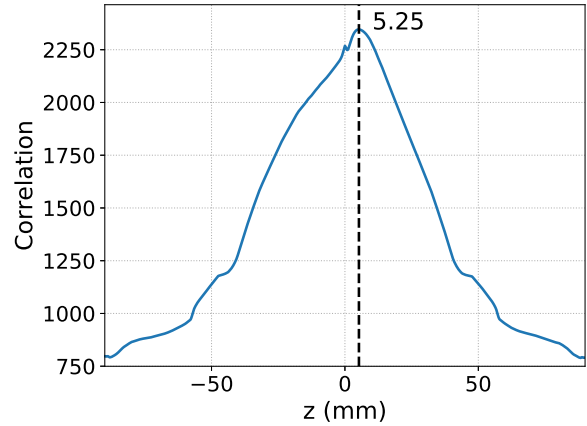


Fig. 6. One of the video frames capturing the flow of the bubbles. The white curves indicate the trace of bubble flow in one frame. The vertical displacement of the bubbles in the calibrated distance is denoted by red double head arrow. The white PVC pipe shows the position of the transmitter.



(a) Average 2-D cross-correlation function of 1200 consecutive video frames. The red dashed line indicates the 1-D cross-correlation function with zero delay at the y-axis.



(b) 1-D cross-correlation function denoting the vertical displacement.

Fig. 7. Visual observation of the air-bubble plume.

IV. CONCLUSION

We have investigated the concept of acoustic scintillation for random sources in an underwater scenario. Through several tank experiments, we demonstrated that the idea of acoustic scintillation with random signals for flow estimation is fea-

TABLE II
SUMMARY OF THE TIME LAG MEASUREMENTS AND THE AVERAGE RISING SPEED ESTIMATES.

	30 kHz	60 kHz	90 kHz	WGN	α SGN	visual
$\tau \times 10^{-3}$ (s)	42	48	54	30 – 70	30 – 70	60
v_z (mm/s)	446	391	347	268 – 625	268 – 625	315

sible. For comparison, experiments were also conducted for deterministic narrowband signals. Rising speed estimates of the air-bubble plume using narrowband and random signals were consistent and also held up with observations recorded by a video camera. For future work, we would like to deploy an array of sensors in Singapore waters to study the performance of flow estimation based on acoustic scintillation with real snapping shrimp noise. As expected, the spatiotemporal variations of snapping shrimp noise will deviate from the random signals deployed in our tank experiment, which given our success with the current work, is worth a study. For instance, snapping shrimp noise is not only a point source in practice but is due to multiple clusters of point sources (snapping shrimp colonies) distributed randomly in space. The collection of turbulent flow ground truth data will definitely be a challenging task during sea trials. In summary, using random signals such as snapping shrimp noise offers an exciting new prospect of estimating the turbulent characteristics in underwater scenarios. This opens up a new opportunity for long-term passive sensing based on acoustic scintillation with ambient noise underwater.

ACKNOWLEDGMENT

The authors would like to acknowledge colleagues at ARL for their support in conducting the tank experiment. We would also like to thank Ms. Ong Lee Lin for proofreading the paper.

REFERENCES

- [1] W. Munk and C. Wunsch, "Ocean acoustic tomography: A scheme for large scale monitoring," *Deep Sea Res.*, vol. 26, no. 2, pp. 123–161, 1979.
- [2] O. A. Godin, N. A. Zaboltn, and V. V. Goncharov, "Ocean tomography with acoustic daylight," *Geophys. Res. Lett.*, vol. 37, no. 13, p. L13605, 2010.
- [3] O. A. Godin, V. V. Goncharov, and N. A. Zaboltn, "Passive ocean acoustic tomography," in *Proc. of Trans. (Dokl) Russ. Acad. Sci., Sect. Earth Sci.*, vol. 444, no. 1, 2012, pp. 606–609.
- [4] V. C. Tsai, "On establishing the accuracy of noise tomography travel-time measurements in a realistic medium," *Geophys. J. Int.*, vol. 178, no. 3, pp. 1555–1564, 2009.
- [5] E. d. Marinis, O. Gasparini, P. Picco, S. Jesus, A. Crise, and S. Salon, "Passive ocean acoustic tomography: theory and experiment," in *Proc. of Eur. Conf. on Underwater Acoust.*, 2002, pp. 497–502.
- [6] V. I. Tatarskii, *Wave propagation in a turbulent medium*. McGraw-Hill, 1961.
- [7] R. W. Lee and J. C. Harp, "Weak scattering in random media, with applications to remote probing," *Proc. IEEE*, vol. 57, no. 4, pp. 375–406, 1969.
- [8] S. F. Clifford and D. M. Farmer, "Ocean flow measurements using acoustic scintillation," *J. Acoust. Soc. Amer.*, vol. 74, no. 6, pp. 1826–1832, 1983.
- [9] D. Di Iorio and D. M. Farmer, "Separation of current and sound speed in the effective refractive index for a turbulent environment using reciprocal acoustic transmission," *J. Acoust. Soc. Amer.*, vol. 103, no. 1, pp. 321–329, 1998.
- [10] M. O. Lammers, R. E. Brainard, W. W. Au, T. A. Mooney, and K. B. Wong, "An ecological acoustic recorder (EAR) for long-term monitoring of biological and anthropogenic sounds on coral reefs and other marine habitats," *J. Acoust. Soc. Amer.*, vol. 123, no. 3, pp. 1720–1728, 2008.
- [11] M. Chitre, S. Kuselan, and V. Pallayil, "Ambient noise imaging in warm shallow waters; robust statistical algorithms and range estimation," *J. Acoust. Soc. Amer.*, vol. 132, no. 2, pp. 838–847, 2012.
- [12] L. A. Chernov and R. A. Silverman, *Wave propagation in a random medium*. McGraw-Hill New York, 1960.
- [13] V. I. Tatarskii, "The effects of the turbulent atmosphere on wave propagation," *Jerusalem: Israel Program for Scientific Translations*, 1971, 1971.
- [14] J. G. Gonzalez, J. L. Paredes, and G. R. Arce, "Zero-order statistics: a mathematical framework for the processing and characterization of very impulsive signals," *IEEE Trans. Signal Process.*, vol. 54, no. 10, pp. 3839–3851, 2006.
- [15] W. L. Haberman and R. K. Morton, "An experimental investigation of the drag and shape of air bubbles rising in various liquids," *David Taylor Model Basin, Rep.* 802, 1953.